Dictyostelium Myosin 25-50K Loop Substitutions Specifically Affect ADP Release Rates†

Coleen T. Murphy and James A. Spudich*

Departments of Biochemistry and Developmental Biology, Stanford University School of Medicine, Stanford, California 94305

Received November 26, 1997; Revised Manuscript Received March 10, 1998

ABSTRACT: While most of the sequence of myosin's motor domain is highly conserved among various organisms and tissue types, the junctions between the 25 and 50 kDa domains and the 50 and 20 kDa domains are strikingly divergent. The 50-20K loop is positioned to interact with actin, while the 25-50K loop is situated nearer the ATP binding site [Rayment, I., et al. (1993) *Science 261*, 50−58]. Chimeric studies of the 50-20K loop [Uyeda, T. Q.-P., et al. (1994) *Nature 368*, 567−569; Rovner, A. S., et al. (1995) *J. Biol. Chem. 270* (51), 30260−30263] have shown that this loop affects actin activation of ATPase activity. Given the function of myosin as a molecular motor, it was proposed that the 25-50K loop might specifically alter ADP release [Spudich, J. A. (1994) *Nature 374*, 515−518]. Here we study the role of this loop by engineering chimeras containing the *Dictyostelium* myosin heavy chain with loops from two enzymatically diverse myosins, rabbit skeletal and *Acanthamoeba*. The chimeric myosins complement the myosin null phenotype in vivo, bind nucleotide normally, interact normally with actin, and display wild-type levels of actin-activated ATPase activity. However, the rate of ADP release from the myosins, normally the slowest step involved in motility, was changed in a manner that reflects the activity of the donor myosin. In summary, studies of *Dictyostelium* myosin heavy chain chimeras have shown that the 50-20K sequence specifically affects the actin-activated ATPase activity [Uyeda, T. Q.-P., et al. (1994)] while the 25-50K sequence helps determine the rate of ADP release.

Myosins are actin-based motors that use the energy of ATP hydrolysis to carry out muscle contraction and a variety of cellular functions, including cytokinesis (*1*, *2*), cell-surface receptor capping (*3*), and developmental processes (*4*). Conventional myosin, or myosin II, has been characterized in many systems, and although myosin isoforms are highly homologous throughout most of the catalytic domain, their enzymatic properties are variable as determined by their ATPase rates and unloaded shortening velocities (*5*).

Structural, biochemical, and biophysical studies of myosin II have allowed predictions to be made about the mechanisms involved in the actin−myosin cycle. One proposal was that two proteolytically sensitive, solvent-exposed loops which were not resolved in the crystal structure (*6*) could be critical for modulating the V_{max} of the ATPase cycle and the maximum velocity of movement (*7*). Proteolysis at these loops divides skeletal myosin S1[1] into three fragments of 25, 50, and 20 kDa (*8*), and Reisler and co-workers showed that proteolysis of the 50-20K loop affects the actin-activated ATPase activity while proteolysis of the 25-50K loop affects motility (*9*). The 50-20K loop, or loop 2, lies in the actin-binding face, and chimeras of *Dictyostelium* myosin with loop 2s from other myosins were found to have actin-activated ATPase activities which correlated with that of the donor myosins (*10*). The 25-50K loop, or loop 1, lies nearer the ATP-binding pocket, and due to this proximity, it is possible that changes in this loop could affect nucleotide binding or product release.

To study the role of loop 1 in the actin−myosin cycle, we have made chimeras of *Dictyostelium* myosin II with loop 1s from *Acanthamoeba* myosin II and rabbit skeletal myosin II. We found that the chimeras' ATPase activities, actin interactions, and nucleotide binding properties are virtually unchanged by loop 1 modifications, while ADP release is affected by these changes in a manner that correlates with the activities of the donor myosins. Interestingly, the limit to the rate of motility of *Dictyostelium* myosin seems to involve two steps, that of ADP release and actin−myosin dissociation, rather than simply ADP release as is the case for vertebrate myosins (*11*). Engineering changes in loop 1 specifically changed the rate of one strongly bound step, ADP release.

MATERIALS AND METHODS

Plasmid Construction. Standard methods were used for all DNA manipulations (*12*), and all myosin vectors encode either full-length or subfragment-1 (S1) of *Dictyostelium* myosin II. Restriction enzymes were from New England BioLabs. A common 3′ oligonucleotide primer encoding a *Sal*I site and individual mutagenic 5′ primers encoding the loop and an *Xba*I site were used with template pLittle-myosin (*13*) to PCR-synthesize 0.2 kb fragments containing the loops: *Sal*I oligo 1, 5′-CACTCAAGAGATGGTCGACATCT-

† This work was supported by NIH Grant 33289 to J.A.S. C.T.M. is a Howard Hughes Medical Institute Predoctoral Fellow.

* To whom correspondence should be addressed at the Department of Biochemistry, SUMC, Stanford, CA 94305. Phone: (650) 723-7634. Fax: (650) 725-6044. E-mail: jspudich@cmgm.stanford.edu.

[1] Abbreviations: S1, subfragment-1; P_i, inorganic phosphate; kb, kilobase; MLCK, myosin light chain kinase; mant, 2′(3′)-*O*-(*N*-methylanthraniloyl).

S0006-2960(97)02903-6 CCC: $15.00
Published on Web 04/22/1998

TCAAAGG-3′; *Acl*I oligo, 5′-GCTCTAGAACACCACCT-(T/G)CATTACGACCAGCGACAGATG-3′; and RBXI oligo, 5′-GCTCTAGAACACCTTGCATTTTA(C/A)CTGGAG-TTGGTTCTTCTTTCTTTTTATCATTACGACCA-GCGACAGATG-3′.

The PCR products were subcloned into pBluescript, sequenced, and then subcloned into the pBIGmyosin vector (*13*) with a unique *Sal*I site in the myosin sequence at nucleotide 487 and a unique *Xba*I site at nucleotide 627. The fragment between the *Sal*I and *Xba*I sites had been replaced with a 950 bp sequence to allow identification of full-length myosin clones containing the proper loop fragments (pBIG-myoA11 and pBIGmyoR11). To create the S1 loop constructs, the pBIGmyosin loop vectors were digested with *Bsa*BI and *Bst*XI, and these 1.5 kb fragments were purified and ligated with the pTIKL-OE-S1-His_6 vector (a generous gift from T. Q.-P. Uyeda) which had been partially digested with *Bsa*BI followed by digestion with *Bst*XI.

Dictyostelium Manipulations. All cells were grown at 22 °C in HL5 medium with 17% FM medium (Gibco BRL), 100 units/mL penicillin, and 100 μg/mL streptomycin. Plasmids were electroporated into HS1, a myosin II null strain (*14*). Transformants were selected for and maintained with 5 μg/mL G418 (Gibco BRL). Cells transformed with the full-length myosin vectors were grown in suspension, while S1-transformed cells were grown on 530 cm^2 Petri dishes (Nunc). Cells were developed on lawns of *Klebsiella aerogenes* on SM/5 agar plates (*15*).

Protein Purification. Full-length myosins (M_r = 500 kDa) were purified from *Dictyostelium* as described by Ruppel et al. (*14*); cells were lysed in low-salt EDTA buffer, extracted with Mg^{2+} ATP, and subjected to two rounds of myosin filament assembly−disassembly. Myosin was treated with bacterially expressed myosin light chain kinase A containing the activating point mutation T166E (*16*) and analyzed by urea−glycerol PAGE (*14*, *17*). The myosin concentration was determined by a Bradford assay (*18*) using rabbit skeletal myosin as a standard.

S1 proteins (M_r = 130 kDa) were purified according to the procedure of Manstein and Hunt (*19*) as modified by Giese and Spudich (*20*). Briefly, cells were washed and depleted of ATP while lysing, and the cytoskeleton was pelleted. The pellet was extracted with Mg^{2+} ATP, and the resulting supernatant was loaded onto a Ni^{2+}-affinity column, washed with 300 mM sodium acetate and then with 30 mM imidazole, and eluted in a 30 to 300 mM imidazole gradient. Fractions were analyzed by SDS−PAGE, pooled, dialyzed against 10 mM HEPES buffer overnight, and loaded onto two 1 mL HiTrap Q columns in series (Pharmacia). The S1 protein eluted in a gradient of 0 to 500 mM KCl and was dialyzed against 25 mM HEPES (pH 7.4), 25 mM KCl, 5 mM $MgCl_2$, and 1 mM DTT (*21*). The concentration was determined spectrophotometrically at 280 nm using an extinction coefficient of 0.8 cm^2/mg. All assays were carried out on at least two preparations of myosin or S1 and are reported as an average of the values.

Actin (M_r = 42 kDa) was purified from chicken skeletal muscle according to the method of Pardee and Spudich (*22*), and the concentration was determined spectrophotometrically using an extinction coefficient of 0.62 cm^2/mg at 290 nm. Phalloidin was added at a slight molar excess to stabilize actin for light scattering experiments.

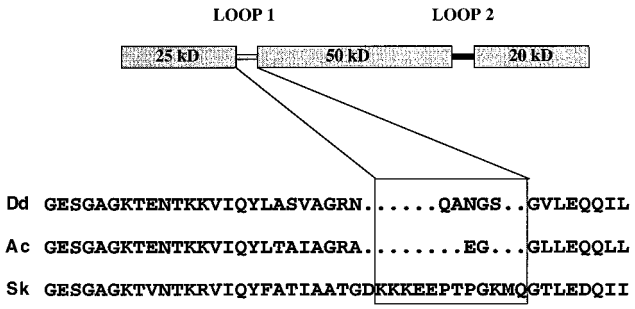

FIGURE 1: Chimera construction. The loop 1 sequence (*5*) of *Dictyostelium* myosin II (in the box) was replaced with the loop 1 sequence from *Acanthamoeba* and rabbit skeletal myosin II by PCR and transformed into *Dictyostelium* myosin null cells.

In Vitro Motility Assays. MLCK-A-treated myosin motility was measured using standard sliding filament assay methods (*23*) at 30 °C. Concentrated myosin was first incubated with 0.2 mg/mL actin and 5 mM ATP and centrifuged to remove dead myosin heads. Myosin (0.8 mg/mL) in assay buffer [AB, 25 mM imidazole (pH 7.4), 25 mM KCl, 4 mM $MgCl_2$, 1 mM EGTA, and 10 mM DTT] was incubated in a flow cell for 2 min before blocking with BSA; unlabeled actin was introduced to block dead myosin heads, and then rhodamine-labeled skeletal F-actin was added, followed by AB/BSA containing 8−10 mM ATP, 0.8% methylcellulose, and an oxygen scavenger system. Actin filaments were tracked at 30 frames/s with a frame grabber board (Scion Corp.), and images were processed using NIH Image, as previously described (*24*).

ATPase Assays. Myosin ATPase activities were determined by measuring release of labeled P_i using [γ-^{32}P]ATP according to the method of Clarke and Spudich (*25*) as modified by Ruppel (*14*). Low-salt Mg^{2+}ATPase reaction mixtures contained 25 mM imidazole (pH 7.4), 25 mM KCl, 4 mM $MgCl_2$, 1 mM DTT, 3 mM ATP, 0.1 mg/mL myosin, and either 0 or 1 mg/mL actin.

Stopped-Flow Spectrophotometry. Stopped-flow experiments were performed at 20 °C with an Applied Photophysics DX.17MV sequential stopped-flow spectrophotometer. Light was provided by an Osram xenon lamp and passed through an Applied Photophysics SpectraKinetic monochromator. Reactions were followed by measurement of 2′(3′)-*O*-(*N*-methylanthraniloyl) nucleotide fluorescence excited at 290 nm and monitored at 90° through a KV 380 nm cutoff filter. Light scattering experiments were performed using an excitation wavelength of 340 nm and monitoring at 90° through a WG 335 cutoff filter. Data were analyzed by a least-squares fitting procedure (Kaleidagraph, Abelbeck Software). Assays were carried out in buffer [25 mM HEPES (pH 7.4), 1 mM DTT, and 5 mM $MgCl_2$] containing either 25 or 100 mM KCl.

RESULTS

Chimera Construction. The sequence of the myosin II head is fairly well-conserved evolutionarily except at two solvent-exposed, flexible loops that vary considerably in size and sequence. Full-length and subfragment-1 constructs of chimeric myosins were created by replacing loop 1 of *Dictyostelium* myosin II with those of *Acanthamoeba* myosin II (pBIG-A11) and rabbit skeletal myosin II (pBIG-R11) (Figure 1), as determined by sequence alignment (*5*). These

Table 1: Summary of Rate Constants of the Interaction of Mant Nucleotides with Rabbit S1, *Dictyostelium* S1, the *Acanthamoeba* Chimera, and the Skeletal Chimera[a]

nucleotide	apparent rate constant	rabbit S1	*Dictyostelium* S1	*Acanthamoeba* chimera S1	skeletal chimera S1
mantATP	$k_{on} \times 10^{-6}$ (M^{-1} s^{-1})	3.2[b]	0.7 ± 0.1	0.7 ± 0.1	0.7 ± 0.1
mantADP	$k_{on} \times 10^{-6}$ (M^{-1} s^{-1})	2.9[b]	0.5 ± 0.1	0.6 ± 0.1	0.6 ± 0.1
mantADP	k_{off} (s^{-1})	0.3	1.5 ± 0.0	1.1 ± 0.1	2.9 ± 0.1
mantADP	k_{off}/k_{on} (μM) (calculated)	0.1	3.0	1.8	4.8

[a] Values were rounded to the nearest 0.1. All measurements in the table were carried out in 100 mM KCl to compare with previously published values, but the mantADP k_{off} was also measured with 25 mM KCl (see the text). [b] Rabbit S1 was used as a control, and results agree with previously published results (*21*).

myosins were chosen because of their range of motile activities; *Acanthamoeba* myosin, with an unloaded sliding velocity of 0.3 μm/s (*26*), may be considered a slow myosin, while skeletal myosin is fast [5−8.8 μm/s (*27*, *28*)] compared to *Dictyostelium* myosin [3 μm/s (*29*)].

The crystal structures of head fragments of both chicken skeletal (*6*) and *Dictyostelium* myosin II (*30*) have been determined, and loop 1 appears to be flexible or to adopt more than one conformation in both proteins, because no electron density could be resolved or modeled for the loop in either structure. The location of these unresolvable loops corresponds well with the assignment of the loop by sequence alignment, and has given us confidence that we have chosen the borders of the loop correctly. Additionally, *Acanthamoeba* myosin's sequence is similar to *Dictyostelium* myosin [about 60% identical (*5*)] except at the loops, allowing the selection of the loop border even in the absence of a crystal structure for *Acanthamoeba* myosin II. Because of the similarity between *Acanthamoeba* and *Dictyostelium* sequences, and the position of the loop borders in the *Dictyostelium* myosin crystal structure, it is likely that the substitution of the *Acanthamoeba* loop is not simply a deletion of the loop.

Loop 1 Chimeras Are Functional in Vivo. *Dictyostelium* cells require myosin for cytokinesis (*1*, *2*) and at two stages of development into fruiting bodies (*31*). Myosin null cells transformed with either of the myosin chimera vectors (pBIG-A11 and pBIG-R11) grew in suspension at normal rates and developed into fruiting bodies, fully complementing the myosin null phenotype. Western blots indicate that expression levels were comparable to the levels of wild-type myosin expression (data not shown). One advantage of the *Dictyostelium* system is that it provides an in vivo test for myosin function; the normal in vivo activities and expression levels showed that the changes at the loops did not cause the protein to become unstable or to fold improperly.

Loop 1 Changes Do Not Affect ATPase Activity. The steady-state rate of ATP hydrolysis by myosin is known to be limited by product release and is stimulated by the addition of actin. ATPase assays were used to determine whether changes at loop 1 affect these activities. Purified myosins were assayed for low-salt Mg^{2+} (basal) and actin-activated ATPase activities at 1 mg/mL actin (Figure 2). Both loop 1 chimeric myosins had basal and actin-activated ATPase activities that were similar to wild-type myosin activities (0.1 and 0.7 s^{-1}, respectively) rather than the activities of the donor myosins (3 s^{-1} with 15 μM actin for *Acanthamoeba* myosin and 20 s^{-1} with 23 μM actin for skeletal heavy meromyosin), indicating that the loop 1 changes have no effect on phosphate release or actin activation. This is in contrast to the loop 2 chimeras, which displayed large changes in actin-activated ATPase activity, including a 5-fold higher ATPase activity at 1 mg/mL actin for the skeletal chimera compared to wild-type *Dictyostelium* myosin (*10*). Thus, changes at the two loops have extremely different effects on ATPase activity.

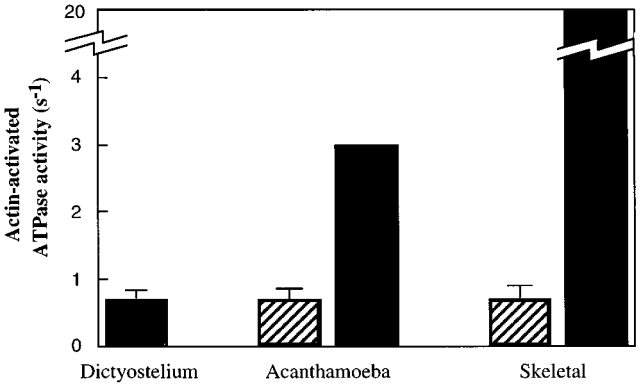

FIGURE 2: Actin-activated ATPase activities of native and loop 1 chimeric myosins. The *Dictyostelium* and chimeric myosins (in hatched bars) display activities near 0.7 s^{-1} with 1 mg/mL actin; the activity of native *Acanthamoeba* myosin is 3 s^{-1} with 0.63 mg/mL actin (*26*), and the rabbit skeletal HMM activity is 20 s^{-1} (*27*). Higher activities have been cited for skeletal myosin (*45*). The value for HMM rather than myosin is quoted because the conditions described are most similar to the conditions used in this study (*10*).

Loop 1 Changes Do Not Affect Nucleotide Binding. 2′(3′)-*O*-(*N*-Methylanthraniloyl), or mant, analogues of ATP and ADP, which display enhanced fluorescence upon binding to myosin subfragment-1 (S1), were used in stopped-flow spectrophotometric assays to determine nucleotide binding rate constants (Table 1). S1 (0.25 μM final concentration) was mixed with 2.5−25 μM mantATP (Figure 3a) or 1.25−7.5 μM mantADP (Figure 3b) (final concentrations), and the fluorescence increase upon mant nucleotide binding was monitored. The second-order rate constants for binding mantATP (7×10^5 M^{-1} s^{-1}) were found to be similar for the chimeras and wild-type S1 and are close to values published previously for *Dictyostelium* S1 (*21*). The two chimeras' mantADP binding constants are equal to that of wild type (about 6×10^5 M^{-1} s^{-1}) within error. In contrast, rabbit S1 binds both mantATP and mantADP with rate constants of 3×10^6 M^{-1} s^{-1} (*21*). We also found that the second-order rate constant of binding of mantATP to the actin−S1 complex (1×10^5 M^{-1} s^{-1}) was not affected by changes in loop 1. Thus, the loop 1 changes do not significantly affect the rate constants of nucleotide binding.

In Vitro Velocity Is Affected by Loop 1 Sequence Changes. The skeletal chimera displayed choppy movement and filament shredding, which usually indicates the presence of

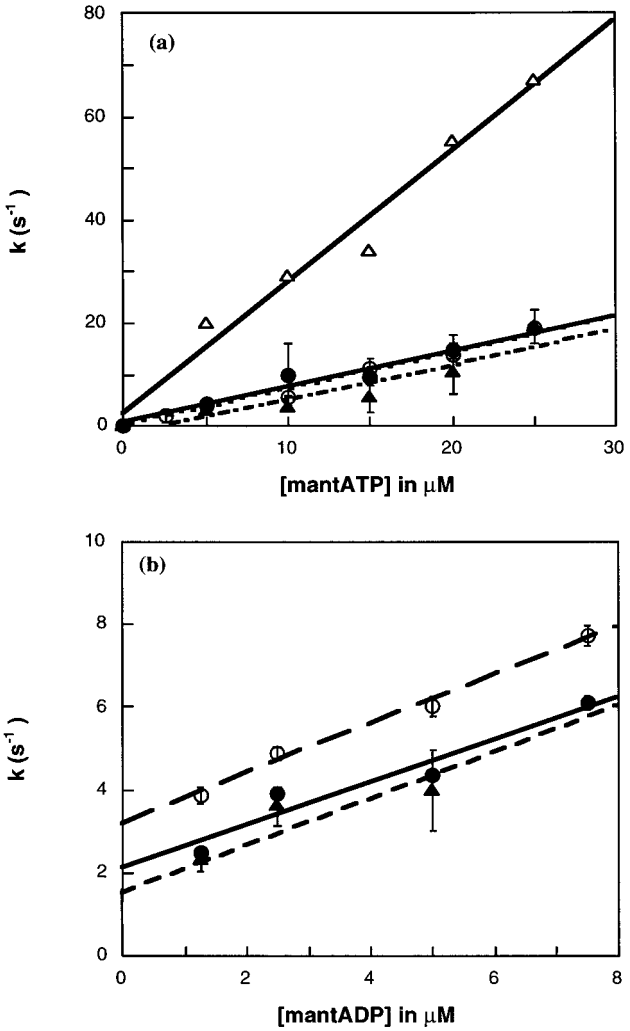

FIGURE 3: Nucleotide interactions with S1 chimeras. (a) MantATP (2.5−25 μM final concentration) was mixed with 0.25 μM S1 (final), and an increase in fluorescence was observed; k_{obs} vs [mant nucleotide] was plotted to obtain the apparent second-order binding constant. In both figures, *Dictyostelium* S1 is designated by filled circles, the skeletal chimera by open circles, and the *Acanthamoeba* chimera by filled triangles, and their rate constants of mantATP binding are 7.0, 7.3, and 6.9 $\times$ 10^5 M^{-1} s^{-1}, respectively. The open triangles in panel a represent rabbit skeletal S1 rates, and the rate constant (2.6 $\times$ 10^6 M^{-1} s^{-1}) is similar to previously published values. (b) MantADP (1.25−20 μM final concentration) was mixed with 0.25 μM S1. The second-order binding constants are 5.2, 5.9, and 5.7 $\times$ 10^5 M^{-1} s^{-1} for *Dictyostelium*, the skeletal chimera, and the *Acanthamoeba* chimera, respectively.

inactive myosin heads; the motility assay is extremely sensitive to these "dead heads" because they bind to actin filaments and create drag. After actin-affinity purification and treatment of bound myosin with unlabeled actin, which removes inactive heads, movement was still not smooth. We obtained an average of 3.0 $\pm$ 0.3 μm/s for the skeletal chimera velocity; the wild-type myosin average was 3.3 $\pm$ 0.6 μm/s, and the *Acanthamoeba* chimera moved smoothly at 1.2 $\pm$ 0.3 μm/s under the same conditions (Figure 4).

MantADP Release Rates Are Altered by Loop 1 Sequence Changes. To determine nucleotide release rates from S1 in the absence of actin, the decrease in fluorescence upon dissociation of S1−mantADP complexes was monitored (Figure 5). Under low-salt conditions (to compare with actin−S1−mantADP release rates described below), *Dictyostelium* S1 released mantADP at a rate of 2.5 $\pm$ 0.1 s^{-1}; the skeletal chimera released mantADP at twice this rate (4.9 $\pm$ 0.4 s^{-1}), and the *Acanthamoeba* chimera's rate was slower than that of the wild type (1.9 $\pm$ 0.1 s^{-1}). Under high-salt conditions (to compare with previously published results), the rates were 1.5, 2.9, and 1.1 s^{-1} for *Dictyostelium* S1, the skeletal chimera S1, and the *Acanthamoeba* chimera S1, respectively (Table 1). Note that the values obtained for k_{off} in this experiment are very close to the values obtained by extrapolation through the *y*-intercept of the mantADP binding slope. Using the values for k_{off} and k_{on}, we determined that skeletal myosin has an approximately 30-

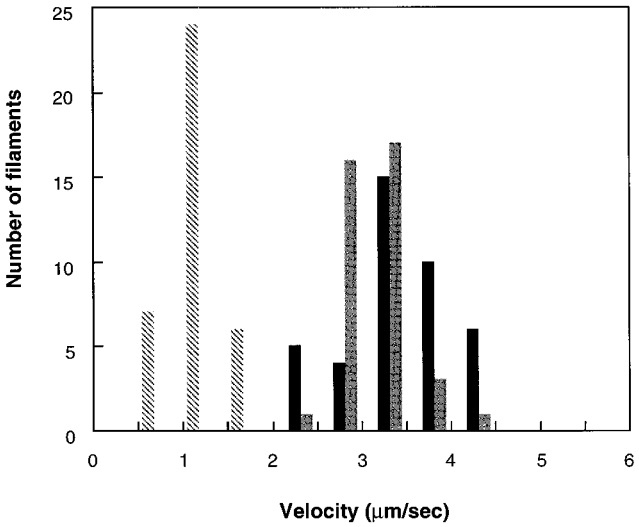

FIGURE 4: Histogram of observed velocities. *Acanthamoeba* chimera, skeletal chimera, and wild-type *Dictyostelium* myosin velocities were measured in the in vitro motility assay at 30 °C, and for each myosin type, about 40 actin filaments were tracked at 30 frames/s using the Scion frame grabber board and then analyzed with NIH Image. Average values $\pm$ standard deviation are as follows: 1.2 $\pm$ 0.3 μm/s for the *Acanthamoeba* chimera (cross-hatched), 3.0 $\pm$ 0.3 μm/s for the skeletal chimera (shaded), and 3.3 $\pm$ 0.6 μm/s for the wild-type *Dictyostelium* myosin (solid).

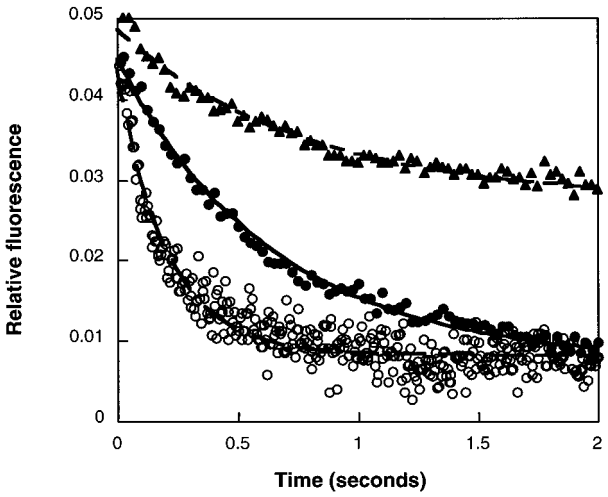

FIGURE 5: MantADP release from S1. S1 (0.5 μM) was preincubated with 2.5 μM mantADP, and the complex was mixed in the stopped-flow device with 80 μM ATP. Shown are sample traces from this experiment done in 100 mM KCl; in these examples, *Dictyostelium* S1 (●) releases mantADP at 1.5 s^{-1}, the skeletal chimera (○) releases at 4.8 s^{-1}, and the *Acanthamoeba* chimera (▲) releases at 1.0 s^{-1}. The wild-type and *Acanthamoeba* chimera traces were fitted to their entire time courses (5 and 10 s, respectively) rather than the 2 s limit shown in the figure.

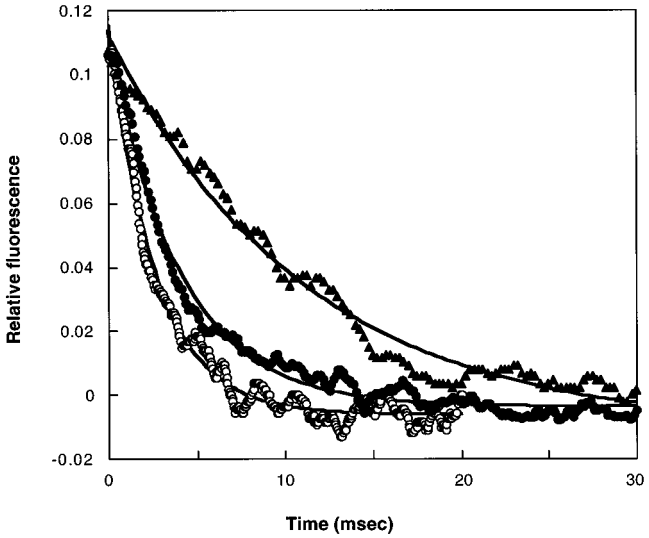

FIGURE 6: MantADP release from actin−S1 at 20 °C. Complexes of 2.5 μM actin, 1 μM S1, and 5 μM mantADP were preformed and allowed to equilibrate, and then these actin−S1−mantADP complexes were rapidly mixed with 20 mM ATP. The excitation wavelength was 290 nm, and fluorescence above 380 nm was monitored. The skeletal chimera released ADP at twice the rate of *Dictyostelium*, and the *Acanthamoeba* chimera's k_{off} was $^1/_3$ of the rate of *Dictyostelium* (Table 2). Representative traces from a series of at least four superimposing traces are shown, with rates of >500, 245, and 89 s^{-1} for the skeletal chimera S1 (○), *Dictyostelium* S1 (●), and the *Acanthamoeba* chimera S1 (▲), respectively. The traces were fitted to their entire time course rather than to the 30 ms limit shown in the figure.

Table 2: MantADP Release from Actin−S1[a]

temperature (°C)	rabbit S1	*Dictyostelium* S1	*Acanthamoeba* chimera S1	skeletal chimera S1
20	>500	250 ± 40	90 ± 14	>500
15	>500	230 ± 50	50 ± 22	480 ± 90

[a] MantADP off rates (s^{-1}) from actin−S1−mantADP complexes were determined at 20 and 15 °C as described in Figure 3.

fold stronger affinity for nucleotide compared to the chimeras or *Dictyostelium* S1 (Table 1).

To determine the release rate in the presence of actin, complexes of actin, S1, and mantADP in low-salt buffer were preformed and allowed to equilibrate; this complex (actin−S1−mantADP) was then rapidly mixed with excess ATP at 20 °C, and the fluorescence decrease as a result of mantADP release from the complex was monitored (Figure 6). Note that we used an excitation wavelength of 290 nm, rather than the methylanthraniloyl excitation wavelength of 345 nm. Under conditions where S1 binds strongly to actin, only a small fraction of the mantADP is bound to actin−S1, resulting in a low relative signal when excited at 345 nm; excitation at 290 nm allows one to look specifically at the mantADP which is bound to S1 and excited through fluorescence energy transfer. The rate of mantADP release from actin−S1 is 2 orders of magnitude higher than the rate of mantADP release from S1 alone, and the rates were significantly different for the loop 1 chimeras and *Dictyostelium* S1 (Table 2). While *Dictyostelium* S1 released mantADP at a rate of 250 s^{-1}, the *Acanthamoeba* chimera released the nucleotide at only 90 s^{-1}. The skeletal chimera displayed rates which were at or above the limits of resolution for the instrument (>500 s^{-1}) at this temperature.

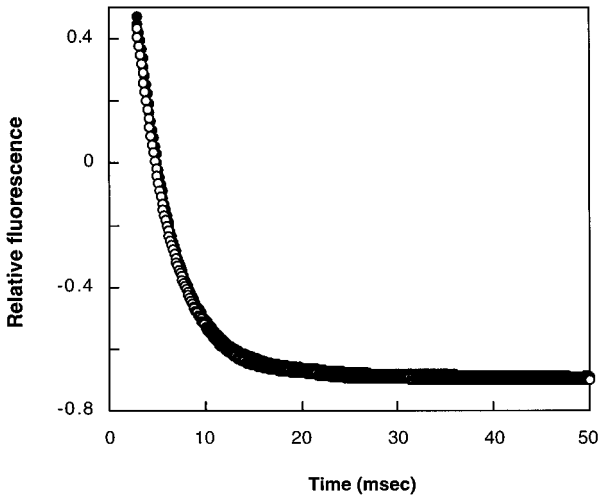

FIGURE 7: Actin−S1 dissociation at 30 °C. Actin−S1 complexes were formed by mixing 2.5 μM phalloidin-stabilized actin with 1 μM S1; dissociation occurred upon mixing with 50 mM Mg^{2+} ATP. Skeletal chimera and wild-type *Dictystostelium* points are shown as open and closed circles, respectively. Traces shown are an average of five consecutive traces and fit to single exponentials. Fits to a single exponential show that both complexes dissociated at 270 s^{-1} at 30 °C.

At 15 °C, the skeletal chimera released mantADP at an average of 480 s^{-1}, while the rates of the wild type and the *Acanthamoeba* chimera slowed to 230 and 50 s^{-1}, respectively. Changes at loop 1 cause the mantADP k_{off} in the presence of actin to drop to $^1/_3$ of the rate of the wild type in the *Acanthamoeba* chimera's case and to double in the skeletal chimera's case. Thus, we have seen both an increase and a decrease in this off rate as a result of changing the loop 1 sequence.

Loop 1 Affects Only One Strongly Bound State. As noted above, changes in the loop 1 sequence did not alter the apparent rate constant of mantATP binding to actin−S1 complexes. Additionally, loop 1 changes did not affect the rate of actin−S1 dissociation, which we measured by adding an excess of ATP to an actin−S1 complex and measuring the change in light scattering as the complex dissociated. At 20 °C in 25 mM KCl, this rate is about 130 ± 20 s^{-1}, which is slower than previously reported [450 s^{-1} (*21*)], but the latter was measured with 100 mM KCl. Therefore, of the three steps associated with strong binding to actin (ADP release, ATP binding, and actin−S1 dissociation), only the rate of ADP release was affected by changes in the loop.

To make valid comparisons with motility data, we carried out stopped-flow assays at 30 °C with 25 mM KCl. We found that the mantADP release rate from wild-type *Dictyostelium* S1 increased to 340 ± 40 s^{-1} at this temperature and the actin−S1 dissociation rate increased to 270 ± 30 s^{-1}, while the rate of mantATP binding remained near 1 × 10^5 M^{-1} s^{-1}. While the mantADP release rate from the skeletal chimera was too fast to measure at 30 °C, the mantATP second-order binding constant and actin−S1 dissociation rate at 30 °C both agreed with values obtained with wild-type *Dictyostelium* S1 (Figure 7), as at 20 °C.

DISCUSSION

In studies of vertebrate muscle myosins, it was shown that unloaded shortening velocity is limited by ADP release from

actin−myosin, and therefore, in vitro velocity measurements are an indirect measure of ADP release rates (*11*). From in vitro sliding velocities, native *Acanthamoeba* myosin [0.34 μm/s (*26*)] would be predicted to release ADP at near $^1/_{10}$ the rate of native *Dictyostelium* myosin, while skeletal myosin [5−8 μm/s (*27*, *28*)] would be expected to release ADP at about twice the rate of *Dictyostelium* myosin. The ADP release rate for skeletal myosin has been estimated to be near 500 s^{-1} (*32*). Although the rate changes we have seen simply as a result of altering the loop 1 sequence indicate that the loop alone does not fully determine the rate of ADP release, the effects of these substitutions on the rate of ADP release, in the absence of any other changes in the rest of the motor, are significant.

Loop 1 may be viewed as a modulator of ADP release from S1. Substituting the loop of *Dictyostelium* myosin with that of *Acanthamoeba* and skeletal myosins causes a decrease and an increase, respectively, in ADP release, both in the presence and in the absence of actin. In the absence of actin, however, skeletal myosin releases mantADP much more slowly than *Dictyostelium* myosin does (0.3 vs 1.5 s^{-1}). It would appear that skeletal myosin is more efficient in its use of nucleotides, binding them strongly until they are activated by actin. Therefore, it is not necessarily surprising that the level of ADP release may be much lower for skeletal myosin than for *Dictyostelium* myosin. Thus, if we could create chimeras of skeletal myosin with the loop 1 of *Dictyostelium* and *Acanthamoeba* myosin, we might expect their activities to be even lower than 0.3 s^{-1}. It is the variation of the activities of the chimeras from the activity of the wild-type *Dictyostelium* myosin which is notable.

Both the in vitro velocity of the *Acanthamoeba* chimera and mantADP release from the actin−chimeric S1 complex are about $^1/_3$ of the rate of the wild type, which is in agreement with the model of Siemankowski and White. However, the skeletal chimera, which releases mantADP at about twice the rate of the wild type, does not show an obvious 2-fold increase in in vitro velocity. In agreement with previous studies, we have found that both the second-order rate constants for ATP binding to actin−*Dictyostelium* S1 (1×10^5 M^{-1} s^{-1}) and actin−*Dictyostelium* S1 dissociation (100−300 s^{-1}) are 1 order of magnitude lower than the values for skeletal S1 (2.5×10^6 M^{-1} s^{-1} and 5000 s^{-1}, respectively). As a result, at physiological ATP concentrations (1−2 mM), the three steps of ADP release, ATP binding, and actin−S1 dissociation are on the same order of magnitude (100−500 s^{-1}). This is quite different from the case of skeletal S1, whose ADP release is much slower than either ATP binding or actin−myosin dissociation. Thus, if ADP release is sped up enough, it should no longer be the rate-limiting step of *Dictyostelium* velocity; instead, the ATP on rate and subsequent actin−myosin dissociation rates, which are not affected by changes in loop 1, may limit velocity, and we would expect to reach a maximum in vitro velocity which is independent of the rate of ADP release. Additionally, if the steps after ADP release and before actin−myosin dissociation are strongly bound, they may cause the "rigor" binding and the subsequent actin filament shredding that we see in the skeletal chimera motility assays. The lengthened ADP-bound state of the *Acanthamoeba* chimera has slowed its motility, while the skeletal chimera's velocity is not increased markedly because the actin−myosin dissociation also contributes to the rate-limiting step of motility.

In this study, we have used the 2′(3′)-*O*-(*N*-methylanthraniloyl) analogues of ATP and ADP to monitor nucleotide binding to and dissociation from the S1 chimeras. MantATP interactions with S1 have been reported to closely mimic those of ATP with S1 (*32*). The affinity of mantADP binding to S1 alone is 10-fold higher than that of ADP binding; however, the affinities of mantADP and ADP binding to actin−S1 are very similar (*32*). Additionally, the ADP−BeF_x component is positioned very similarly in the crytal structures of *Dictyostelium* S1 bound to Mg^{2+}−mantADP−BeF_x (*33*) and Mg^{2+}−ADP−BeF_x (*30*). Therefore, it is not unreasonable to assume that changes in loop 1 which affect mantADP release from actin−S1 also affect the ADP release rate in the same manner.

While the results reported here are the first direct measurements of rates of mantADP release from myosin loop chimeras, studies of alternatively spliced smooth muscle myosin and scallop myosin (*34*) have shown that changes at loop 1 affect in vitro motility (*35*) and thus possibly ADP release, but changes in ATPase rates were seen as well. It is not clear whether the differences in results are due to the type of myosin used as the host, the expression systems used, the borders of the loops chosen, or the nature of the loops themselves. Our studies have shown that changes at loop 1 of *Dictyostelium* myosin cause changes in ADP release in a manner that correlates with the activity of the donor myosin, while having little effect upon ATPase activity. It has been observed previously that there is no direct correlation between actin-activated MgATPase activity and in vitro motility (*7*, *8*, *11*, *36*). A proteolytic study of rabbit skeletal HMM (*9*) showed that independent cleavage of loop 1 and loop 2 affects motility and ATPase activity separately, supporting the idea that the loops can independently affect these rate-limiting steps of the cycle.

Although these loops are generally considered to be nonconserved, a study of the sequences of the loops revealed that change in the loops is actually suppressed in myosins with similar kinetics (H. V. Goodson, H. Warrick, and J. A. Spudich, in preparation). The loops may have provided a site for evolutionarily fine-tuning the activity of the motor through changes in enzymatic activities or regulation. In fact, Rovner et al. (*37*) have found that changes at loop 2 disrupt regulation of smooth muscle myosin.

It is not apparent how loop 1 functions to alter ADP release. Studies of glutathione synthetase (*38*), dihydrofolate reductase (*39*), pancreatic lipase (*40*), chymotrypsin and trypsin (*41*), and other enzymes with flexible loops (*42*) have shown that short stretches of amino acids are able to protect substrates from bulk solvent, expose catalytic groups upon reorientation, stabilize intermediates, define substrate specificity, and determine the flexibility of active sites. Biophysical studies will be necessary to determine the mechanism by which loop 1 may be affecting myosin kinetics. Our study does not eliminate the possibility that length, rather than sequence, determines the rate of ADP release; we will address that issue by creating additional chimeras with long loops from slow myosins.

Previously regarded as simple linkers of highly conserved sequences, solvent-exposed, nonconserved loops are now considered to be important in modulating the kinetics of enzymatic reactions (*41*, *43*, *44*). Studies of the loops of

myosin have shown that these linker peptides may in fact be important for modifying kinetics to optimize an isoform for a particular function without altering conserved catalytic residues.

ACKNOWLEDGMENT

We thank R. Cooke's and M. Geeves' laboratories for gifts of mant nucleotides, M. Geeves for his help with the initial stopped-flow experiments, T. Uyeda for expression plasmids, K. Giese for valuable discussion, M. Heideker for assistance with NIH Image, and H. Warrick, K. Giese, S. Nock, and W. Shih for reviewing the manuscript.

REFERENCES

1. Knecht, D. A., and Loomis, W. F. (1987) *Science 236*, 1081−1086.
2. De Lozanne, A., and Spudich, J. A. (1987) *Science 236*, 1086−1091.
3. Pasternak, C., Spudich, J. A., and Elson, E. L. (1989) *Nature 341*, 549−551.
4. Peters, D. J., Knecht, D. A., Loomis, W. F., De, L. A., Spudich, J., and Van, H. P. (1988) *Dev. Biol. 128*, 158−163.
5. Sellers, J. R., and Goodson, H. V. (1995) in *Motor proteins 2: myosin* (Sheterline, P., Ed.) Vol. 2, pp 1323−1423, Academic Press Limited, London.
6. Rayment, I., Rypniewski, W. R., Schmidt-Base, K., Smith, R., Tomchick, D., Benning, M. M., Winkelmann, D. A., Wesenberg, G., and Holden, H. (1993) *Science 261*, 50−58.
7. Spudich, J. A. (1994) *Nature 372*, 515−518.
8. Mornet, D., Pantel, P., Audemard, E., and Kassab, R. (1979) *Biochem. Biophys. Res. Commun. 89*, 925−932.
9. Bobkov, A. A., Bobkova, E. A., Lin, S.-H., and Reisler, E. (1996) *Proc. Natl. Acad. Sci. U.S.A. 93*, 2285−2289.
10. Uyeda, T. Q.-P., Ruppel, K. M., and Spudich, J. A. (1994) *Nature 368*, 567−569.
11. Siemankowski, R. F., Wiseman, M. O., and White, H. D. (1985) *Proc. Natl. Acad. Sci. U.S.A. 82*, 658−662.
12. Sambrook, J., Fritsch, E. F., and Maniatis, T. (1989) *Molecular Cloning. A Laboratory Manual*, Cold Spring Harbor Laboratory Press, Cold Spring Harbor, NY.
13. Patterson, B., and Spudich, J. A. (1995) *Genetics 140*, 505−515.
14. Ruppel, K. M., Uyeda, T. Q.-P., and Spudich, J. A. (1994) *J. Biol. Chem. 269*, 18773−18780.
15. Sussman, M. (1987) in *Cultivation and synchronous morphogenesis of Dictyostelium under controlled experimental conditions* (Spudich, J. A., Ed.) pp 9−29, Academic Press, Inc., Orlando, FL.
16. Smith, J. L., Silveira, L. A., and Spudich, J. A. (1996) *EMBO J. 15*, 6075−6083.
17. Perrie, W. T., Smillie, L. B., and Perry, S. V. (1973) *Biochem. J. 131*, 151−156.
18. Bradford, M. M. (1976) *Anal. Biochem. 72*, 248−254.
19. Manstein, D. J., and Hunt, D. M. (1995) *J. Muscle Res. Cell Motil. 16*, 325−332.
20. Giese, K. C., and Spudich, J. A. (1997) *Biochemistry 36*, 8465−8473.
21. Ritchie, M. D., Geeves, M. A., Woodward, S. K. A., and Manstein, D. J. (1993) *Proc. Natl. Acad. Sci. U.S.A. 90*, 8619−8623.
22. Pardee, J. D., and Spudich, J. A. (1982) *Methods Cell Biol. 24*, 271−289.
23. Uyeda, T. Q.-P., Kron, S. J., and Spudich, J. A. (1990) *J. Mol. Biol. 214*, 699−710.
24. Heidecker, M., and Marriott, G. (1996) *Biochemistry 35*, 3170−3174.
25. Clarke, M., and Spudich, J. A. (1974) *J. Mol. Biol. 86*, 209−222.
26. Ganguly, C., Baines, I. C., Korn, E. D., and Sellers, J. (1992) *J. Biol. Chem. 267*, 20900−20904.
27. Toyoshima, Y. Y., Kron, S. J., McNally, E. M., Niebling, K. R., Toyoshima, C., and Spudich, J. A. (1987) *Nature 328*, 536−539.
28. Lowey, S., Waller, G. S., and Trybus, K. M. (1993) *Nature 365*, 454−456.
29. Uyeda, T. P.-Q., Abramson, P. D., and Spudich, J. A. (1996) *Proc. Natl. Acad. Sci. U.S.A. 93*, 4459−4464.
30. Fisher, A. J., Smith, C. A., Thoden, J. B., Smith, R., Sutoh, K., Holden, H., and Rayment, I. (1995) *Biochemistry 34*, 8960−8972.
31. Springer, M. L., Patterson, B., and Spudich, J. A. (1994) *Development 120*, 2651−2660.
32. Woodward, S. K. A., Eccleston, J. F., and Geeves, M. A. (1991) *Biochemistry 30*, 422−430.
33. Bauer, C. B., Kuhlman, P. A., Bagshaw, C. R., and Rayment, I. (1997) *J. Mol. Biol. 274*, 394−407.
34. Perreault-Micale, C. L., Kalabokis, V., Nyitray, L., and Szent-Györgyi (1996) *J. Muscle Res. Cell Motil. 17*, 543−553.
35. Rovner, A. S., Freyzon, Y., and Trybus, K. (1997) *J. Muscle Res. Cell Motil. 18*, 103−110.
36. Umemoto, S., and Sellers, J. R. (1990) *J. Biol. Chem. 265*, 14864−14869.
37. Rovner, A. S., Freyzon, Y., and Trybus, K. M. (1995) *J. Biol. Chem. 270*, 30260−30263.
38. Kato, H., Tanaka, T., Yamaguchi, H., Hara, T., Nishioka, T., Katsube, Y., and Oda, J. (1994) *Biochemistry 33*, 4995−4999.
39. Gekko, K., Kunori, Y., Takeuchi, H., Ichihara, S., and Kodama, M. (1994) *J. Biochem. 116*, 34−41.
40. Jennens, M. L., and Lowe, M. E. (1994) *J. Biol. Chem. 269*, 25470−25474.
41. Hedstrom, L., Szilagyi, L., and Rutter, W. (1992) *Science 255*, 1249−1253.
42. Kempner, E. S. (1993) *FEBS Lett. 326*, 4−10.
43. DiBella, E. E., and Scheraga, H. A. (1996) *Biochemistry 35*, 4427−4433.
44. First, E. A., and Fersht, A. R. (1995) *Biochemistry 34*, 5030−5043.
45. Wagner, P. D. (1981) *J. Biol. Chem. 256*, 2493−2498.

BI972903J